Active interactions between turbulence and bed load: Conceptual picture and experimental evidence

Alessio Radice,[1] Vladimir Nikora,[2] Jenny Campagnol,[1] and Francesco Ballio[1]

[1] This paper reports results from experiments with simultaneous measurement of areal bed-load sediment concentration and water velocity (horizontal and vertical components) made at 1.5 particle diameters above the mean bed. The same spatial and temporal scales were employed to measure the kinematic properties of flowing water and sediments. The obtained data, covering a range of low sediment discharges, were analyzed in terms of bulk statistics, autocorrelation and cross-correlation functions, and quadrant decomposition of fluctuations. At the lowest transport rates, the motion of sediment particles was found to be mostly associated with sweep events. However, with increasing flow rate and bed-load discharge, the process mechanics changed, and the transport of sediments was also found to be significantly correlated with ejections. The obtained results are integrated into a conceptual picture attempting to bridge previous depictions of the bed-load transport mechanics.

Citation: Radice, A., V. Nikora, J. Campagnol, and F. Ballio (2013), Active interactions between turbulence and bed load: Conceptual picture and experimental evidence, Water Resour. Res., 49, doi:10.1029/2012WR012255.

1. Introduction

[2] The traditional approach to sediment transport has been aimed at the prediction of expected transport rates at the given bulk hydrodynamic conditions [e.g., Shields, 1936; Einstein, 1937, 1950; Meyer-Peter and Müller, 1948; Van Rijn, 1984] (for review see, for example, Graf, [1996]). Such predictions, however, often suffer from significant uncertainty for both the incipient sediment motion and the bed-load discharges [e.g., Buffington and Montgomery, 1997; Buffington, 1999; Gomez and Church, 1989; Martin, 2003]. The latest research efforts, therefore, have been directed toward a more detailed description of grain motion with the purpose of developing, in the long term, advanced mechanism-based models of sediment transport.

[3] A dependence of the transport process on turbulence has been proven through experimentation. For example, Sumer et al. [2003] mentioned that "The sediment transport increases markedly with increasing turbulence level." Some models incorporating velocity fluctuations in predicting incipient motion have been proposed [e.g., Zanke, 2003; Vollmer and Kleinhans, 2007]. Furthermore, over recent decades, researches have proven the existence of coherent structures spanning in scale from small near-bed eddies to structures occupying the entire flow depth and with the longitudinal extension of many depths [e.g., Kline et al., 1967; Grass, 1971; Nezu and Nakagawa, 1993; Shvidchenko and Pender, 2001; Detert et al., 2010; Marusic et al., 2010]. It has thus been proposed that these structures should play a significant role in particle dislodgement and transport [e.g., Grass, 1970; Jackson, 1976; Drake et al., 1988; Mazumder, 2000]. Therefore, several experimental works have been devoted to seeking a relationship between the events of the burst cycle and particle entrainment and motion. These studies cover a range of experimental conditions and approaches (small/coarse particles, hydraulically smooth/rough flows, fixed/loose underlying sediment bed, measurement of kinematics of both phases or one of them) and have highlighted a variety of mechanisms for the sediment transport. For example, Rashidi et al. [1990] and Niño and García [1996] attributed a major role in sediment entrainment to fluid ejections from the bed; Nelson et al. [1995] suggested that sweeps impinging the bed and outward interactions are most probable agents for the transport of sediments; Drake et al. [1988], Cameron [2006], Dwivedi et al. [2010], and Dey et al. [2011] indicated sweeps as major transporting events, whereas Sechet and Le Guennec [1999] hypothesized a double effect involving both sweeps and ejections; and Papanicolaou et al. [1999, 2001] attributed the major role to the streamwise velocity components, as representative of the drag force acting on particles. Many of these studies suffered from a scale mismatch in measurement techniques used for assessing flow fields and sediment motion. For example, Nelson et al. [1995] employed one-point Laser Doppler Anemometry (LDA) measurements for flow velocity that were compared with a line-averaged solid discharge; and Sechet and Le Guennec [1999] used one-point LDA measurements for flow velocity, while sediment dynamics was evaluated using Lagrangian tracking of moving particles, thus making

[1]Dipartimento di Ingegneria Civile e Ambientale, Politecnico di Milano, Milan, Italy.

[2]School of Engineering, University of Aberdeen, Aberdeen, Scotland, UK.

Corresponding author: A. Radice, Dipartimento di Ingegneria Civile e Ambientale, Politecnico di Milano, Piazza L. da Vinci 32, I-20133 Milan, Italy. (alessio.radice@polimi.it)

conclusions based on inconsistent temporal scales of turbulent events and particle resting times.

[4] According to the brief literature review presented above, recent studies have brought valuable new information and highlighted several questions that remain presently unanswered. Among these are the following: (1) Is it feasible to link sediment transport to a particular turbulent event? (2) Does the mechanism of sediment transport change with the change of the bulk flow parameters and sediment properties (as it seems from earlier results)? and (3) Is it possible to show that different findings represent different facets of a larger picture? The goal of this paper is to report results from one consistent set of experiments, trying to address these research questions. This paper continues research on bed-load sediment transport mechanisms along the lines of statistical descriptions of Radice and Ballio [2008], Radice [2009], and Radice et al. [2009, 2010]. The distinctive feature of the present work is the focus on the interaction between flow turbulence and the bed sediment transport process. This paper is structured as follows. First, laboratory experiments are described where we have tried to achieve a scale consistency for flow and sediment measurements. Then, the experimental findings are enumerated, and a synoptic interpretation of the obtained data is attempted, completing this paper with final conclusions.

2. Experiments

[5] The experiments used in this paper were conducted at the Hydraulic Engineering Laboratory of the Politecnico di Milano. A pressurized, transparent, 5.8 m long duct with 0.40 m wide and 0.16 m high cross section was used for the experiments. Approximately midway along the duct, a recess section was installed and filled with quasi-circular polyvinyl chloride (PVC) cylinders of the specific gravity 1.43 (i.e., the ratio of particle density to the water's one). These particles were used instead of spheres because of their easy availability (such PVC grains are typically produced as semimanufactured materials for several industrial applications). A characteristic size of the sediments was determined as the diameter of a sphere having the same volume as a PVC particle; this size equals to 3.6 mm and, in the following, will be referred to as d. In the remaining parts of the duct, the particles were glued to the bed surface to ensure homogeneity in bed roughness. The measurement section was 4.8 m (or 60 duct half-heights) downstream from the duct entrance where the flow was expected to be fully developed or at least nearly fully developed. The experimental setup was similar to that in Radice et al. [2009].

[6] During each run, a video camera was used to film particle movements, whereas a package of two ultrasonic velocity profilers (UVPs) was employed to measure the streamwise (u) and vertical (w) components of water velocity at an elevation of 5.3 mm above the mean sediment bed. The UVPs were oriented at 75 in relation to the (horizontal) flow direction and were also used to obtain the time-averaged profiles of streamwise velocity, with up to 80 bins, each 2 mm thick and 10–12 mm wide. The quasi-instantaneous bed-load sediment concentration (C) was measured from the images using the method of Radice et al. [2006]. A spatial averaging area of 3.5 cm 3.5 cm was used for the measurement of particle concentration and

was selected to satisfy two requirements: (1) to be consistent with the extension of the UVP ultrasonic beam at the bed level and (2) to be appropriate for the Eulerian analysis of sediment concentration with a resolution much finer than the section-averaged characterization. The latter is justified by the fact that the size of the averaging area used in our study was much larger than the particle size but much smaller than the flow scale. Duration of each experiment was around 180 s, with the same sampling frequency of 25 Hz for both water velocity and sediment concentration. Radice et al. [2009] provided arguments justifying use of this sampling frequency for a full capture of large-scale structures and partial resolution of smaller-scale, short-lived turbulent events. The spatial equivalent of the measurement duration of 180 s, obtained using Taylor's frozen turbulence hypothesis, was equal to 600–900 flow half depths or approximately to 100–200 lengths of large-scale eddies. This value is intermediate between those used in the field [Nikora and Goring, 2000] and laboratory [Dey et al., 2012] experiments. Based on our assessments and these studies, the standard errors increase from 2%–4% for first-order moments to 6%–9% for the second-order moments.

[7] As pointed out by Radice et al. [2009], the described experimental setup, representative of covered flows, differs from free-surface flows typically studied in sediment transport research. The literature on sediment transport indicates that transport mechanisms in covered flows are not significantly different from those in free-surface flows, while definitions of the threshold conditions for both flow types are conceptually the same (see, for example, a review by Ettema, [2008]). The bed-load equations developed for open-channel flows may also be used for covered flows, provided the ratio of the shear stress to its threshold value is appropriately estimated. Therefore, the outcomes of our study may have direct applicability to both free-surface and covered flows.

[8] The characteristics of the experimental tests are shown in Table 1 and Figure 1. The bulk Reynolds Re and Froude Fr numbers were computed using the duct height and cross-sectional mean velocity, whereas the grain Reynolds number Re* is based on the particle size and shear velocity. The latter was computed from UVP time-averaged profiles of streamwise velocity, using the following equation:

$$\frac{u(z)}{u_*} = \frac{1}{\kappa} \ln \frac{z}{d} + B, \tag{1}$$

where u is the time-mean velocity at elevation z, u* is the shear velocity, is the von Karman constant (a value of

Table 1. Characteristics of the Experimental Tests

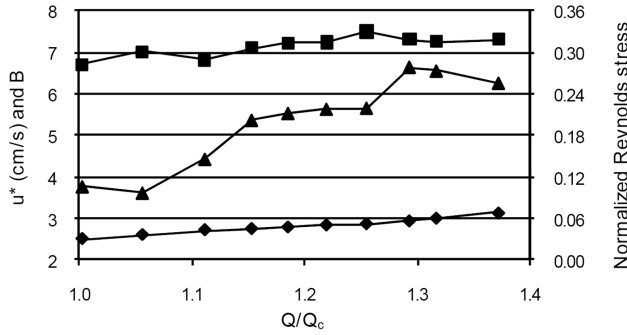| Test	Q (L/s)	Re		Fr	Q/Q_c	u* (cm/s)	Re*
1	19.0	4.7	10^4	0.25	1.003	2.50	90
2	20.0	5.0	10^4	0.26	1.056	2.60	94
3	21.1	5.3	10^4	0.28	1.111	2.72	98
4	21.8	5.5	10^4	0.29	1.153	2.75	99
5	22.5	5.6	10^4	0.29	1.185	2.79	100
6	23.1	5.8	10^4	0.30	1.219	2.84	102
7	23.8	5.9	10^4	0.31	1.255	2.87	103
8	24.5	6.1	10^4	0.32	1.293	2.94	106
9	25.0	6.2	10^4	0.33	1.317	3.01	108
10	26.0	6.5	10^4	0.34	1.372	3.14	113

Figure 1. Flow parameters for a range of studied flow rates at the duct symmetry plane: diamonds ¼ u*; squares ¼ B; triangles ¼ $\overline{u^{0}w^{0}}$=u ^{2} at z ¼ 5.3 mm.

0.40 was used), and B is a parameter representing the ratio of flow velocity to the shear velocity at z ¼ d, i.e., B ¼ u(d)/u*. The origin z ¼ 0 was found based on the vertical profile of the echo received by the UVPs; the obtained velocity profiles fitted a logarithmic formula within the range from z ¼ 15 to 60 mm. The threshold discharge for incipient motion of the experimental sediments was Q_c ¼ 18.95 L/s, as previously measured by Radice and Ballio [2008]. The ratio Q/Q_c (analogous to the shear velocity ratio u*/u*$_c$) ranged from 1.0 to 1.4 in our experiments that together with the condition Re* > 90 (Table 1) enabled the studied flows to be defined as weakly mobile, rough-bed flows. The short duration of the experiments prevented the bed elevation to lower significantly during the runs, even in the absence of sediment feeding.

[9] The flow parameters at the duct symmetry plane for the range of studied flow rates are depicted in Figure 1. The change of the shear velocity is approximately linear with the discharge, as one would expect bearing in mind a constant friction factor for a range of studied Re (i.e., u* uf$^{0.5}$ Qf$^{0.5}$, where f is Darcy-Weisbach friction factor). The parameter B increases with increasing water discharge, apparently toward an asymptotic value of approximately 7.3. A possible interpretation of slight variation of B at smaller Q/Q_c relates to particle mobility. Indeed, the ratio u(d)/u* may grow with increasing number of rolling/sliding particles, and, thus, B should also increase. An attainment of a saturation value of B at approximately Q/Q_c ¼ 1.25 (Figure 1) may be due to a diminishing effect of the particle concentration C on the parameter B after C exceeds some threshold value. The primary Reynolds stress at z ¼ 5.3 mm, normalized on the squared shear velocity (i.e., $\overline{u^{0}w^{0}}$=u ^{2}), varied in our experiments from approximately 0.10 at the lowest flow rate to 0.25 at the highest flow rate. This range (0.10–0.25) is much lower than one would expect for the two-dimensional (2-D) flow over fixed rough bed where it should be around 0.9 or even higher. The observed discrepancy is likely due to the combined effect of several factors, related to both flow mechanics and the measurement limitations in our experiments. First, it could be explained by an effect of a "weakly mobile bed" for which the von Karman constant may be less than the conventional value of 0.40 used in the present estimates of the shear velocity (i.e., smaller von Karman constant would lead to smaller values of the shear velocity and thus to higher $\overline{u^{0}w^{0}}$=u ^{2}). For

open-channel flows, such an effect was reported by Nikora and Goring [2000] and Dey et al. [2012] and could be one of the reasons of low values of the normalized Reynolds stress in this study. The second factor, contributing to the reduced values of $\overline{u^{0}w^{0}}$=u ^{2}, can relate to inherent secondary currents, which in duct flows are typically stronger than in free-surface flows [e.g., Nezu and Nakagawa, 1993]. Third, the reduced ratio $\overline{u^{0}w^{0}}$=u ^{2} may also reflect the smoothing effect of the UVP sampling volume, i.e., the reduction of measured values of $\overline{u^{0}w^{0}}$ as a result of filtering out contributions to $\overline{u^{0}w^{0}}$ from the eddies comparable to the sizes of the sampling volume (whose size is minimum 5 mm 10 mm 4 mm).

3. Results

[10] The research findings in this section are presented in relation to (1) bulk statistics of bed-load sediment concentration, (2) autocorrelation properties of the flow and sediment quantities, and (3) water-sediment interaction processes assessed using cross correlation and quadrant analysis techniques.

3.1. Bulk Statistics of Bed-Load Sediment Concentration

[11] The basic statistics of concentration (mean and coefficient of variation, with the latter being the ratio of standard deviation to mean) are shown in Figure 2a as a function of the test discharge. Furthermore, a comparison of the
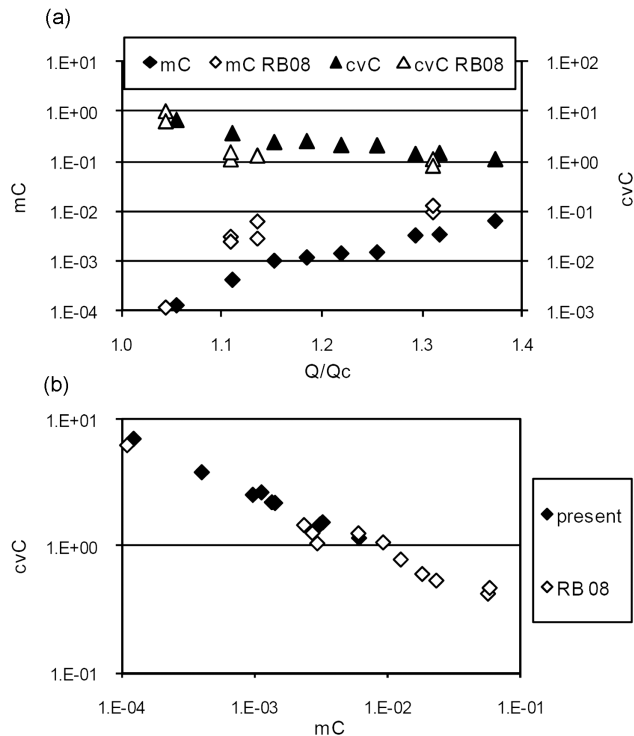

Figure 2. (a) Time-averaged value (mC) and coefficient of variation (cvC) of sediment concentration for a range of water discharges. (b) Relationship between time-averaged concentration and coefficient of variation. Present data are compared with those of Radice and Ballio [2008], denoted as RB08.

present data with those of Radice and Ballio [2008] is also presented. The new data are generally consistent with the earlier experiments, even though some points show lower mean values and higher irregularity (represented by the coefficient of variation) than those of Radice and Ballio [2008] for similar Q/Q_c. In this respect, it should be noticed that the configuration of the experimental duct was not exactly the same in the two studies. In the present tests, the duct inlet was equipped with a flow aligner that was not present in the earlier experiments. The aligner might have reduced the turbulence of the flow arriving at the recess section. It has been indeed found in the literature [e.g., Sumer et al., 2003] that the turbulence level of a flow may significantly influence the sediment transport rate measured for a given flow discharge. Figure 2b presents a comparison between the previous and the new data in terms of correlation between the first-order and second-order statistics, which yields a good collapse of data. It may thus be argued that the relationship between water discharge and sediment concentration is influenced by the incoming turbulence, whereas the effect of the inlet flow condition on a relationship between the time-mean concentration and concentration fluctuations is hardly recognizable.

3.2. Autocorrelation Patterns

[12] The cross-correlation function for two generic stationary random functions X_i and X_j can be computed as follows:

$$R_{X_i X_j}(\tau) = \frac{\overline{X_i'(t) X_j'(t + \tau)}}{\sigma_{X_i} \sigma_{X_j}}; \qquad (2)$$

where a prime superscript indicates an instantaneous deviation from the mean value, t is the time argument, τ is the time lag, σ_{X_i} is the standard deviation of X_i (analogously for X_j), and the overbar denotes time averaging. For $i = j$, the autocorrelation function, $R_X(\tau)$, is obtained. The functions $R_X(\tau)$ for $X = u$ at $z = 5.3$ mm and $X = C$ are depicted in Figures 3a and 3b for all tests (gray curves), showing very little differences between the curves for different experiments (i.e., for different sediment transport intensities). This result is in agreement with that found by Radice et al. [2010], who evaluated the characteristic time scales of bed-load sediment concentration at various locations within a duct bed where a significant sidewall effect was observed (the latter led to a transverse variability of the sediment transport intensity comparable to that obtained from experiments with different discharges). In the present case, the similarity of the $R_X(\tau)$ curves for different flow discharges enabled average curves for u, w (both at $z = 5.3$ mm), and C to be used for the following analyses.

[13] The autocorrelation time scales of u, w, and C (estimated as first crossings of average $R_X(\tau)$ with the time axis, Figure 3c) are similar, being of the order of about 1 s. Yet, there are some noticeable differences between the autocorrelation functions for u, w, and C at small time lags, with the autocorrelation of w being lowest and that of C being highest. The high autocorrelation of concentration at small time lags may be related to larger inertia of sediment particle clouds compared to water.
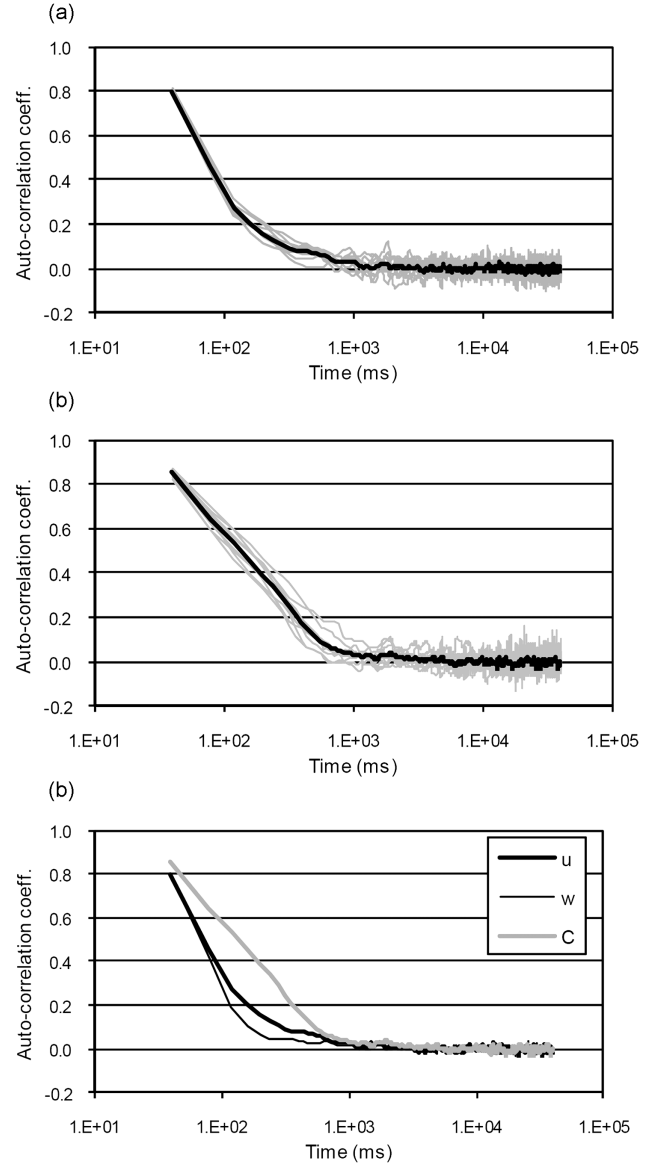

Figure 3. Autocorrelation functions for (a) streamwise velocity component; (b) sediment concentration, curves for all tests in gray and an average curve in black; and (c) average autocorrelation functions for u, w, and C.

3.3. Turbulence-Sediment Interactions

[14] Several methods may be used to evaluate and visualize the interrelations between flow turbulence and bed-load sediment motion. In the following, analyses by means of cross-correlation functions and quadrant-based decomposition of turbulent fluctuations are presented.

[15] The cross-correlation functions between velocity components u and w at $z = 5.3$ mm, and C are depicted in Figure 4. As with the autocorrelation functions, the cross-correlation curves have been averaged over all tests to obtain mean representative curves (see examples in Figures 4a and 4b). Figure 4c shows the averaged cross correlations u-w, u-C, and w-C.

[16] The cross-correlation function between u and w attains a minimum at zero time lag where it is equal, by definition, to their conventional correlation coefficient (which
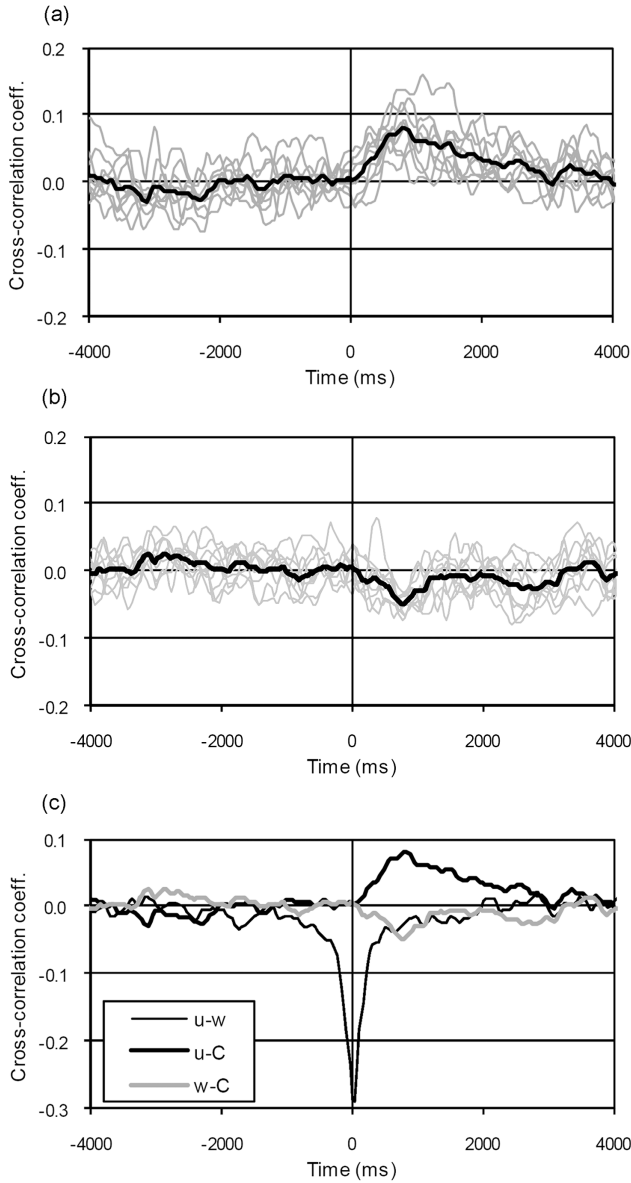
(a)

(b)

(c)

Figure 4. Cross-correlation functions for (a) streamwise velocity component and C; (b) vertical velocity component and C, curves for all tests in gray and average curve in black; and (c) average cross-correlation functions for u-w, u-C, and w-C.

is the primary Reynolds stress normalized on standard deviations of u and w). Its value is around 0.3 (Figure 4c) and is comparable to those reported for near-bed regions in channel flows [Nezu and Nakagawa, 1993]. The cross correlation between the sediment concentration and streamwise velocity component is negligible at zero time lag but increases with increase in the lag reaching a maximum at the lag of approximately 0.9 s. The cross-correlation u^2-C (not shown here, but likely representative of the effect of drag acting on particles) is almost the same as that for u-C. Finally, the cross-correlation curve for w and C is essentially a mirror reflection of the correlation between u and C, with a minimum also occurring at around 0.9 s. Negative correlation between w and C was also found by Radice et al. [2009].

While interpreting these results (see below), it should however be kept in mind that the three cross correlations u-w, u-C, and w-C depend on each other. During the data analysis, we realized that the time lag corresponding to the maximum correlation of u and C and the minimum correlation in w and C might actually vary with the transport intensity, but it was fairly difficult to detect a clear tendency with confidence (that is the reason why all curves are presented without distinction in Figure 4). Therefore, in the following, the (constant) average value of the time lag of extreme correlations will be considered as representative (a possible relation of this time lag to expected characteristic scales of coherent structures in the flow is suggested in section 4).

[17] The second approach of coupling flow velocity and sediment concentration is based on quadrant decomposition and is known as quadrant analysis. This technique, previously used mainly for velocity fields, employs separation of the velocity fluctuations into four groups (i.e., quadrants) depending on the combination of signs of u^0 and w^0, where a prime defines deviation of an instantaneous value from the time-averaged quantity. These quadrants (also known as turbulent events) are as follows: Q1, outward interactions when both u^0 and w^0 are positive; Q2, ejections with $u^0 < 0$ and $w^0 > 0$; Q3, inward interactions when both u^0 and w^0 are negative; and Q4, sweeps with $u^0 > 0$ and $w^0 < 0$. Several data sets are available for the relative occurrence of the turbulent events. They show that sweeps and ejections occur, on average, for around 30% of time each, whereas outward and inward interactions occupy approximately 20% of time each (Table 2). These estimates relate to the near-bed region. In the upper flow layers, the time contributions of all four quadrants tend to be equal [e.g., Keshavarzy and Ball, 1997; Nikora and Goring, 2000]. The estimates from this study, obtained from the UVP measurements at z ¼ 5.3 mm, are summarized in Figure 5. The time occurrence of the events (Figure 5a) varied with the water discharge, attaining values consistent with those in the literature for the largest discharges used. To identify possible effects of particular events on sediment transport, the approach proposed by Nelson et al. [1995] was applied, i.e., the quadrant analysis was repeated considering only velocity samples associated with sediment motion and also lagged by 0.9 s, obtained from the cross-correlation analysis (this strategy was preferred to simple resampling of velocities corresponding to C > 0 that produced less clear result). Figure 5b shows that the Q1 and Q3 events remain approximately the same as in Figure 5a, while conditioning velocity values based on the presence of sediment motion decreased the time occurrence of Q2 and increased it for Q4. This simple analysis highlights a major correlation between sweeps (i.e., Q4) and sediment motion, particularly for the lowest transport conditions investigated. By contrast, for the largest discharge used, the data points in Figures 5a and 5b are similar. The time occurrence of all event types

Table 2. Relative Occurrence of Events Within the Burst Cycle

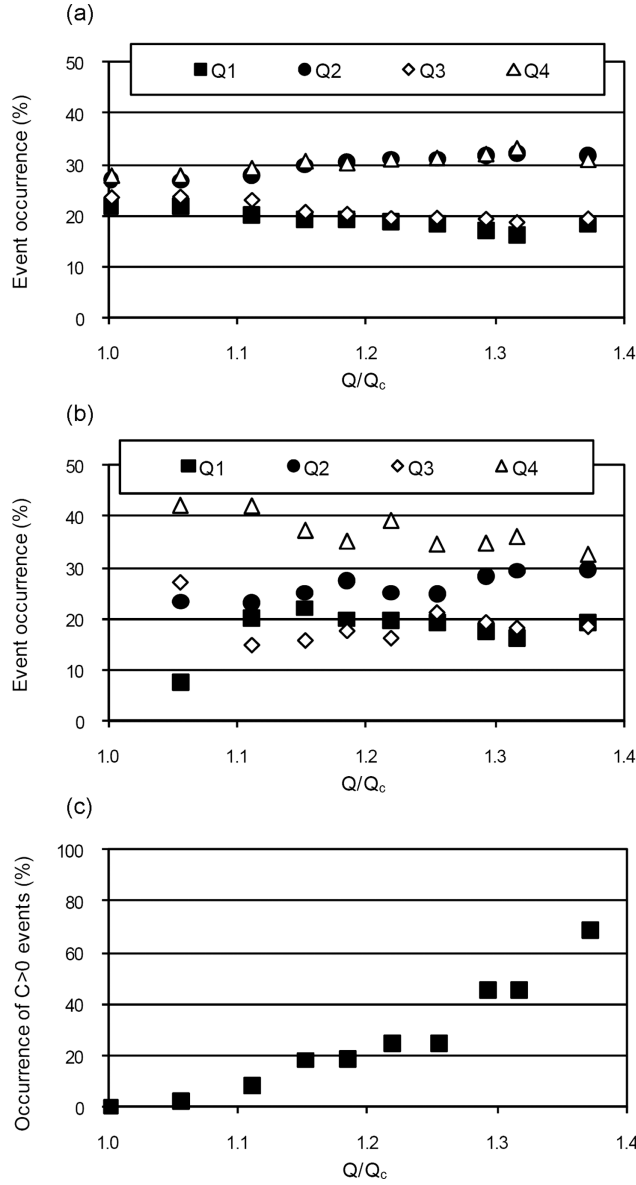| Source	% Q1	% Q2	% Q3	% Q4
Nelson et al. [1995]	16	35	17	31
Keshavarzy and Ball [1997]	20	30	20	30
Nezu and Nakagawa [1993]		29 ⎨ 1.2		34 ⎨ 0.8

(a)

(b)

(c)

Figure 5. (a) Event occurrence; (b) event occurrence considering only time periods when C > 0 and the time lag of 0.9 s obtained from the cross-correlation analysis; and (c) percentage of velocity values associated with sediment motion (C > 0).

with C > 0 (shown in Figure 5b) is depicted for reference in Figure 5(c); the presented percentage is a parameter complementary to the intermittency factor defined by Radice and Ballio [2008] and, as expected, increases with increasing discharge.

[18] Some detailed quadrant analyses for selected tests (test 3, low transport; test 6, intermediate transport; and test 10, high transport) are depicted in Figure 6. Left plots represent the three-dimensional (3-D) relationship u^0-w^0-C. On the right, pictures show the probability density functions (pdfs) of u^0 and w^0, together with a 2-D plot of fluctuations (contour lines proportional to point density). For all tests, data for C ¼ 0 were discarded (this being the reason for increasing point number with increasing test discharge),

and a lag of 0.9 s between water velocity and sediment concentration was implemented. The results show that, for test 3, the highest concentration values are correlated with sweep events (i.e., u^0 > 0, w^0 < 0, as shown by points' density being highest for Q4 of the 2-D plot of fluctuations in Figure 6). Then, as discharge and sediment transport intensity increase, the relationship between velocity fluctuations and sediment concentration tends to become symmetric. Indeed, the pdfs of u^0 and w^0 (with C > 0 and lagged time) for test 10 are almost symmetric. The detected transition from low-transport to high-transport tests is the same as already highlighted in a different way in Figure 5.

4. Synthesis and Discussion

[19] The experimental data described above can be summarized as follows: (i) the characteristics of velocity fluctuations changed with increasing discharge, as shown by the increasing value of the normalized Reynolds stress and by variable time occurrences of the events within the burst cycle (although these effects could also be partially explained by the smoothing effect of the UVP sampling volume); (ii) a negative (expected) cross correlation between u and w, a positive correlation between u and C, and a negative correlation between w and C were detected, with extreme values occurring at a time lag of approximately 0.9 s for correlations between velocity components and concentration; and (iii) at the lowest transport intensities, the sediment motion was mostly correlated with sweep events, whereas, at higher water discharges (and correspondingly higher bed shear stresses), sweep and ejection events were equally correlated with particle motion. These findings are discussed below in light of the research questions posed at the beginning of this paper.

[20] The brief review of existing literature in section 1 shows that a variety of possibilities have been identified in terms of the transport-inducing mechanisms for sediments. The results outlined in the present study have proven, on one hand, a positive correlation between sediment motion and the streamwise velocity component, which could be expected, in principle, bearing in mind a relation between drag forces and streamwise velocity. On the other hand, a significant correlation between sweeps and sediment motion has been reliably detected, particularly at low transport intensities. The two findings are likely representing different facets of the same mechanism, since sweeps are associated with strong positive fluctuations of the streamwise velocities.

[21] Our findings do not highlight ejections as the events mostly correlated with sediment motion, although this may be the case for different experimental conditions. In this respect, it may be noted that Nelson et al. [1995], who documented major role of sweeps and outward interactions, worked with bed shear stresses that were two times higher than a threshold value (i.e., comparable to our highest discharge). On the other hand, Niño and García [1996], based on their transitionally rough-bed experiments, indicated ejections as a major transport mechanism, having values of the Shields parameter larger than 0.25 (i.e., five to six times higher than a threshold value). Our results might bridge these findings. Indeed, our experiments have shown that the prevailing correlation of sediment transport with sweeps decreases with increasing discharge (or bed shear stress),
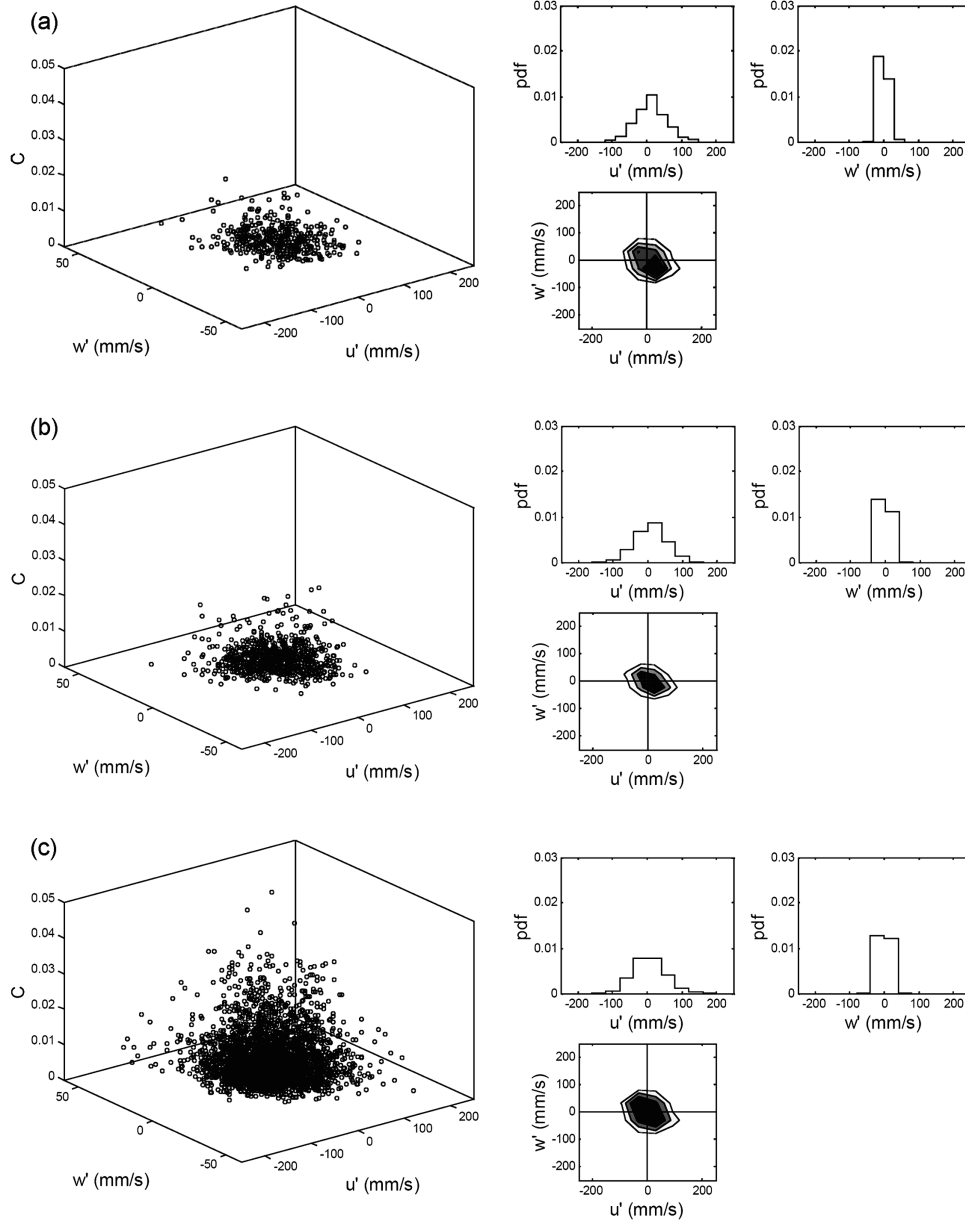
Figure 6. (left) The 3-D plots of the relationship u'-w'-C. (right) Polar plots of u'-w' represented by contour lines of point density and amplitude analysis (pdf) of the u' and w' fluctuations. Tests (a) 3, (b) 6, and (c) 10.

suggesting that the mechanism of sediment transport changes with the bulk flow or transport intensity. This can be explained assuming that, at low flows, only the extreme velocity events are responsible for particle motion [consistently, for example, with proposal of Grass, 1970], whereas, for higher flows, a wider range of velocities has the ability to move sediments. Also, with increase in the concentration of moving particles, the particle-particle interactions become stronger, leading to self-enhancement of grain motion. This interpretation is indeed consistent with a picture where, for bed shear stresses significantly exceeding the threshold, sediment transport is a continuous process with "smooth" statistics [see, for example, Ancey et al., 2008; Radice, 2009], and the bulk-averaged velocities may be appropriately representative of the process. Unfortunately, the range

of transport conditions used in our study was not sufficiently wide for a proper estimation of a "critical" value that separates these two regimes.

[22] The next issue to discuss is the lag of 0.9 s detected between velocity and concentration fluctuations. Roy et al. [2004] provided a review of works in which the size of coherent structures has been measured, highlighting that their characteristic length typically varies between 1 and 6 flow depths. If half the duct height is considered as flow depth, then the estimated streamwise dimension of the coherent structures in our study ranges from 8 to 50 cm. We may assume that the structure length L was 25 cm, while its convection velocity was 25 cm/s, i.e., similar to the average value of u in the tests. The second assumption is just a rough approximation; for example, Radice et al. [2009]
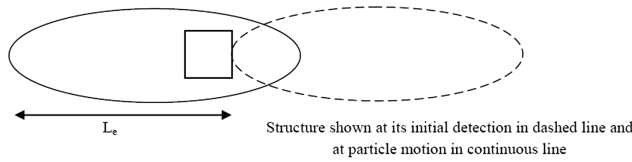
Figure 7. Phenomenological sketch 1. Sediment motion triggered in the tail of the coherent structure. Flow from right to left.

showed that the signature of a large coherent structure on the mobile sediment bed propagated downstream with a higher speed than the near-bed average water velocity. However, this difference should not affect the semiquantitative interpretations shown hereafter. Figure 7 presents a conceptual sketch, including a (fixed) measuring cell with side s and a migrating coherent structure. When the structure passes over the cell, the time over which its signature covers the cell is $T = (L + s)/u$, where u is the convection velocity. Assuming that $s = 4$ cm, $L = 25$ cm, and $u = 25$ cm/s, we can find that $T > 1$ s. Now, several scenarios may be hypothesized according to which a lag between water velocity and sediment concentration will emerge. First, it can be assumed that the sediments are activated by an inner part of the structure (or even its end part), not by its front (Figure 7). In other words, some effective length L_e of the structure has to pass over the cell before particle motion is triggered. On one hand, this is consistent with potential effects of the particle inertia and the force impulse concept [Diplas et al., 2008; Celik et al., 2010; Valyrakis et al., 2011]. On the other hand, some pressure drop occurring within the body of the structure may also be invoked as a potential triggering factor [e.g., Detert et al., 2010]. According to this picture, $L_e = 22$ cm would justify the lag of 0.9 s. A second potential scenario is that the sediments entrained by a certain structure upstream of the cell will reach it with some time delay, due to lower sediment velocity compared to that of water (Figure 8). In this context, the temporal lag is $dt = t_3 - t_2 = D/u_s - D/u$ (u_s is particle velocity). Although a range of possible distances D may contribute to the cross correlation between water velocity and concentration, its maximum is most likely formed by highly coherent sediment "clouds" that may be characterized by a "dispersion scale" comparable to the flow depth. Assuming from previous experiments [Radice and Ballio, 2008] that $u_s = 10$ cm/s, it can be

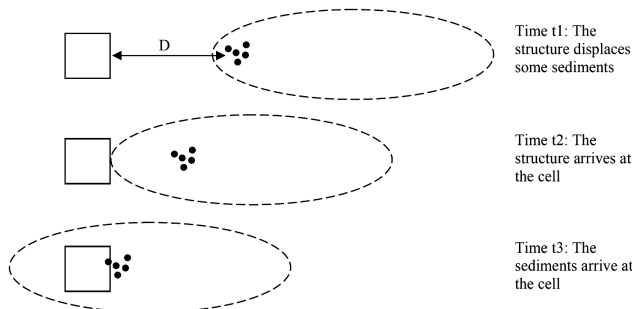obtained that $D = 0.9 \times 250/15 = 15$ cm. Recent estimates by Radice and Ballio [2010] support this value. Finally, a combination of these two scenarios may also be considered (Figure 9). In this more general case, the following relationships are relevant: $t_2 - t_1 = (D - L_e)/u$ and $t_3 - t_2 = [D - u_s(t_2 - t_1)]/u_s = D/u_s - (D - L_e)/u$. Several combinations of L_e and D may lead to $t_3 - t_2 = 0.9$ s. Examples of such combinations are as follows: $L_e = 10$ cm and $D = 8$ cm; $L_e = 8$ cm and $D = 10$ cm; $L_e = 5$ cm and $D = 12$ cm; and $L_e = 0$ cm and $D = 15$ cm.

[23] The presented results may help in the advancement of mathematical and computational models of the sediment transport process. On one hand, they can be used for validation of the models that employ statistical measures of flow-sediment interactions. On the other hand, they can improve physical content of such models by incorporating a temporal lag between the fluctuations of flow velocity and sediment concentration as well as a change in the transport mechanisms with increasing flow intensity.

[24] The work reported in this paper suffers from some limitations that are listed below and that will be addressed in the follow-up studies. First, the water velocity was measured at a single elevation from the bed. It is possible that some findings of this paper would have stronger (or weaker) support if a different measuring elevation was used, a possibility highlighted by Radice et al. [2009]. Second, the UVP sampling volume for velocity measurements is a disk. On one hand, it is consistent with the quasi-two-dimensionality of the bed-load process and with the necessary higher resolution in the vertical direction, along which velocity and concentration gradients are strongest. On the other hand, it could lead to some biases in our estimates (e.g., the normalized Reynolds stress has been shown to vary with water discharge, i.e., with Re). Third, due to experimental constraints, the support scale of concentration and flow measurements was fixed to a certain value that could not be optimal for our analysis. Another potential issue that is worth mentioning is the Eulerian measurement of the sediment concentration employed in our study. In fact, $C > 0$ at a fixed location may mean either that something is being entrained or that something is already moving, e.g., coming from a section upstream of the measuring area. Therefore, the correlation between fluctuations of velocity and C may not be only due to the entrainment process. A Lagrangian measurement of sediment motion (presently under development) will allow to directly correlate flow velocity and entrainment events. Finally, spatially distributed measurements will be needed to properly test the hypothesized sketches in Figures 7–9 to

Figure 8. Phenomenological sketch 2. Sediment motion triggered by coherent structure upstream of the cell. Flow from right to left.
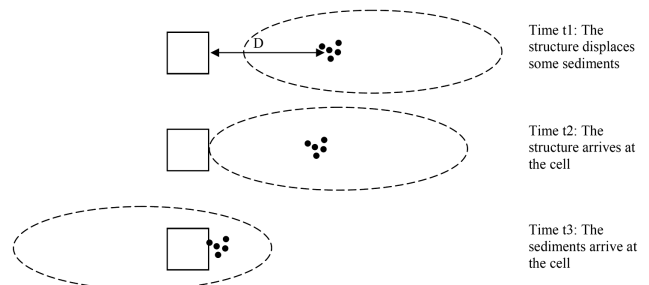

Figure 9. Phenomenological sketch 3. Combination of sketches 1 and 2. Flow from right to left.

interpret the value of the temporal lag between velocity and concentration.

5. Conclusions

[25] Bed-load sediment concentration and water velocity above the granular bed were measured in laboratory experiments for a range of flow rates and bed-load discharges. Maximum bed shear stress tested was equal to 1.9 times the threshold for incipient sediment motion. The distinctive feature of the experimental campaign was the match between the support scales used for the measurement of water and sediment kinematics, a condition that was often neglected in earlier studies of the bed-load process.

[26] The main results of this study can be summarized as follows:

[27] 1. Sediment concentration and horizontal and vertical velocity components display similar autocorrelation patterns. In addition, positive and negative cross correlations were detected between u and C and between w and C, respectively, reflecting the expected properties of the near-bed flow structure.

[28] 2. The turbulent event mostly correlated with sediment transport was not the same for the whole range of studied flow rates. In particular, at the lowest transport rates, the sediment motion events were mostly associated with sweeps. For the highest flow intensities, the correlations of sweeps and ejections with the transport process were similar.

[29] 3. The detected change of the sediment transport dynamics at increasing flow rate frames the results in a conceptual picture that bridges existing findings from the literature. The latter highlighted a variety of mechanisms, likely due to different transport conditions investigated.

[30] 4. The concentration fluctuations exhibit a significant temporal delay compared to those of water velocity. Potential transport mechanisms were hypothesized to support the value of the measured time lag. Spatially distributed velocity measurement and Lagrangian tracking of sediment particles are needed to corroborate these conceptual considerations.

References

Ancey, C., A. C. Davison, T. Böhm, M. Jodeau, and P. Frey (2008), Entrainment and motion of coarse particles in a shallow water stream down a steep slope, J. Fluid Mech., 595, 83–114.

Buffington, J. M. (1999), The legend of A.F. Shields, J. Hydraul. Eng., 125, 376–387.

Buffington, J. M., and D. R. Montgomery (1997), A systematic analysis of eight decades of incipient motion studies, with special reference to grave-bedded rivers, Water Resour. Res., 33, 1993–2029.

Cameron, S. M. (2006), Near-boundary flow structure and particle entrainment, Ph.D. dissertation, The Univ. of Auckland, Auckland, New Zealand.

Celik, A. O., P. Diplas, C. L. Dancey, and M. Valyrakis (2010), Impulse and particle dislodgement under turbulent flow conditions, Phys. Fluids, 22, 046601.

Detert, M., V. Nikora, and G. H. Jirka (2010), Synoptic velocity and pressure fields at the water-sediment interface of streambeds, J. Fluid Mech., 660, 55–86.

Dey, S., S. Sarkar, and L. Solari (2011), Near-bed turbulence characteristics at the entrainment threshold of sediment beds, J. Hydraul. Eng., 137, 945–958.

Dey, S., R. Das, R. Gaudio, and S. K. Bose (2012), Turbulence in mobile-bed streams, Acta Geophys., 60, 1547–1588, doi:10.2478/s11600-012-0055-3.

Diplas, P., C. L. Dancey, A. O. Celik, M. Valyrakis, K. Greer, and T. Akar (2008), The role of impulse on the initiation of particle movement under turbulent flow conditions, Science, 322, 717–720.

Drake, T. G., R. L. Shreve, W. E. Dietrich, P. J. Whiting, and L. B. Leopold (1988), Bedload transport of fine gravel observed by motion-picture photography, J. Fluid Mech., 192, 193–217.

Dwivedi, A., B. Melville, and A. Y. Shamseldin (2010), Hydrodynamic forces generated on a spherical sediment during entrainment, J. Hydraul. Eng., 136, 756–769.

Einstein, H. A. (1937), Der geschiebebetrieb als wahrscheinlichkeitsproblem, Verlag Rascher, Zurich, Switzerland.

Einstein, H. A. (1950), The bed-load function for sediment transportation in open channel flows, Tech. Bull. U. S. Dept. of Agric., 1026, U. S. Dept. of Agric., Washington, D. C.

Ettema, R. (2008), Ice effects on sediment transport in rivers, in Sedimentation Engineering, edited by M. H. Garc a, ASCE Manual Rep. on Eng. Pract. No. 110, pp. 613–648, ASCE, Restion, Va.

Gomez, B., and M. Church (1989), An assessment of bed load sediment transport formulae for gravel bed rivers, Water Resour. Res., 25, 1161–1186.

Graf, W. H. (1996), Hydraulics of Sediment Transport, Water Resources, Colo.

Grass, A. J. (1970), Initial instability of fine bed sand, J. Hydraul. Div., 96, 619–632.

Grass, A. J. (1971), Structural features of turbulent flow over smooth and rough boundaries, J. Fluid Mech., 50, 233–255.

Jackson, R. G. (1976), Sedimentological and fluid-dynamic implications of the turbulent bursting phenomenon in geophysical flows, J. Fluid Mech., 77, 531–560.

Keshavarzy, A., and J. E. Ball (1997), An analysis of the characteristics of rough bed turbulent shear stresses in an open channel, Stoch. Hydrol. Hydraul., 11, 193–210.

Kline, S. J., W. C. Reynolds, F. A. Schraub, and P. W. Rundstadler (1967), The structure of turbulent boundary layer, J. Fluid Mech., 30, 741–773.

Martin, Y. (2003), Evaluation of bed load transport formulae using field evidence from the Vedder River, British Columbia, Geomorphology, 53, 75–95.

Marusic, I., B. J. McKeon, P. A. Monkewitz, H. M. Nagib, A. J. Smits, and K. R. Sreenivasan (2010), Wall-bounded turbulent flows at high Reynolds numbers: Recent advances and key issues, Phys. Fluids, 22, 065103, doi:10.1063/1.3453711.

Mazumder, R. (2000), Turbulence-particle interactions and their implications for sediment transport and bedform mechanics under unidirectional current: Some recent developments, Earth Sci. Rev., 50, 113–124.

Meyer-Peter, E., and R. Müller (1948), Formulas for bed-load transport, in Proceedings of the Second Meeting of IAHR, Stockholm, Sweden, 39–64.

Nelson, J. M., R. L. Shreve, S. R. McLean, and T. G. Drake (1995), Role of near-bed turbulence in bed load transport and bed form mechanics, Water Resour. Res., 31, 2071–2086.

Nezu, I., and H. Nakagawa (1993), Turbulence in Open-Channel Flows, Balkema, Rotterdam, Netherlands.

Nikora, V., and D. Goring (2000), Flow turbulence over fixed and weakly mobile gravel beds, J. Hydraul. Eng., 126, 679–690.

Niño, Y., and M. Garc a (1996), Experiments on particle-turbulence interactions in the near-wall region of an open channel flow: Implications for sediment transport, J. Fluid Mech., 326, 285–319.

Papanicolaou, A. N., P. Diplas, M. Balakrishnan, and C. L. Dancey (1999), Computer vision technique for tracking bed load movement, J. Comp. Civ. Eng., 13, 71–79.

Papanicolaou, A. N., P. Diplas, C. L. Dancey, and M. Balakrishnan (2001), Surface roughness effects in near-bed turbulence: Implications to sediment entrainment, J. Eng. Mech., 127, 211–218.

Radice, A. (2009), Use of the Lorenz curve to quantify statistical nonuniformity of sediment transport rate, J. Hydraul. Eng., 135, 320–326.

Radice, A., and F. Ballio (2008), Double-average characteristics of sediment motion in one-dimensional bed load, Acta Geophys., 56, 654–668, doi:10.2478/s11600-008-0015-0.

Radice, A., and F. Ballio (2010), Coherent particle motion in bed load, in Proceedings of the First Congress of the European Section of IAHR, Edinburgh, U. K.

Radice, A., S. Malavasi, and F. Ballio (2006), Solid transport measurements through image processing, Exp. Fluids, 41, 721–734, doi:10.1007/s00348-006-0195-9.

Radice, A., F. Ballio, and V. Nikora (2009), On statistical properties of bed load sediment concentration, Water Resour. Res., 45, W06501, doi:10.1029/2008WR007192.

Radice, A., F. Ballio, and V. Nikora (2010), Statistics and characteristic scales for bed load in a channel flow with sidewall effects, Acta Geophys., 58, 1072–1093, doi:10.2478/s11600-010-0020-y.

Rashidi, M., G. Hestroni, and S. Banerjee (1990), Particle-turbulence interaction in a boundary layer, Int. J. Multiphase Flow, 16, 935–949.

Roy, A. G., T. Buffin-Belanger, H. Lamarre, and A. D. Kirkbride (2004), Size, shape and dynamics of large-scale turbulent flow structures in a gravel-bed river, J. Fluid Mech., 500, 1–27.

Sechet, P., and B. Le Guennec (1999), Bursting phenomenon and incipient motion of solid particles in bed-load transport, J. Hydraul. Res., 37, 683–696.

Shields, A. (1936), Anwendung der Aehnlichkeitsmechanik und der Turbulenz Forschung auf die Geschiebebewegung, Mitt. der Preussische Versuchanstalt für Wasserbau und Schiffbau, no. 26, Tech. Hochsch., Berlin, Germany.

Shvidchenko, A. B., and G. Pender (2001), Macroturbulent structure of open-channel flow over gravel beds, Water Resour. Res., 37, 709–719.

Sumer, B. M., L. H. Chua, N. S. Cheng, and J. Freds e (2003), Influence of turbulence on bed load sediment entrainment, J. Hydraul. Eng., 129, 585–596.

Valyrakis, M., P. Diplas, and C. L. Dancey (2011), Entrainment of coarse grains in turbulent flows: An extreme value theory approach, Water Resour. Res., 47, W09512, doi:10.1029/2010WR0102236.

Van Rijn, L. C. (1984), Sediment transport, part I: Bed load transport, J. Hydraul. Eng., 110, 1431–1456.

Vollmer, S., and M. G. Kleinhans (2007), Predicting incipient motion, including the effect of turbulent pressure fluctuations in the bed, Water Resour. Res., 43, W05410, doi:10.1029/2006WR004919.

Zanke, U. C. E. (2003), On the influence of turbulence on the initiation of sediment motion, Int. J. Sediment Research, 18, 17–31.